Kinetic Characterization of a Bacteriophage T4 Antimutator DNA Polymerase†

Ping Wu,‡,§ Nancy Nossal,|| and Stephen J. Benkovic*,‡

Department of Chemistry, The Pennsylvania State University, 414 Wartik Laboratory, University Park, Pennsylvania 16802, and National Institute of Diabetes, Digestive & Kidney Disease, Building 8, Room 2A-19, Bethesda, Maryland 20892

Received April 14, 1998; Revised Manuscript Received August 20, 1998

ABSTRACT: Fidelity of DNA replication by bacteriophage T4 DNA polymerase is achieved in a multiplicative process: base selection by its polymerase activity and removal of misincorporated nucleotides by its exonuclease activity. The wild-type polymerase is capable of maintaining a balance between the two activities so that DNA replication fidelity is maximized without excessive waste of nucleotides. Antimutator enzymes exhibit a higher DNA replication fidelity than the wild-type enzyme, at the cost of increased nucleotide turnover. The antimutator A737V polymerase has been characterized kinetically using pre-steady-state and steady-state methods to provide a kinetic sequence which defines the effect of the mutation on the discrete steps controlling DNA replication fidelity. Comparison of this sequence to that of the wild type [Capson, L. T., Peliska, J. A., Kaboord, B. F., Frey, M. W., Lively, C., Dahlberg, M., and Benkovic, S. J. (1992) *Biochemistry 31,* 10984−10994] revealed that A737V polymerase differs in two ways. The rates at which DNA is transferred between the exonuclease and polymerase sites are reduced approximately 7-fold for a duplex DNA containing a mismatched 3′-terminus, and the partitioning of the mismatched duplex between the polymerase and exonuclease sites is 1:2 versus 4:1 for the wild-type enzyme. The exonuclease activity of A737V relative to the wild-type enzyme is unchanged on single-stranded DNA. However, the difference in partitioning the duplex DNA between the exonuclease and polymerase active sites results in an enhanced exonuclease activity for the antimutator enzyme.

T4 DNA polymerase is the central component of a multienzyme complex responsible for replication of the viral genome. The polymerase (the product of gene 43) possesses its 5′−3′ polymerase and 3′−5′ exonuclease activities (*2, 3*) on a single polypeptide chain. The enzyme is one of the least error-prone polymerases known, exhibiting a frequency of misincorporation in vivo of 1 in 10^8 turnovers (*4, 5*). Fidelity arises from a multiplicative process. First, base selection by the polymerase activity provides an error frequency of one misincorporation per 10^5−10^6 turnovers. Second, proofreading by the 3′−5′ exonuclease activity reduces the error frequency a further 10^2−10^3-fold (*6*−*8*). The interplay between polymerase and exonuclease activities is critical in providing high DNA replication fidelity without excessive turnover of nucleotides.

The complete three-dimensional structure of T4 polymerase is not available; however, the crystal structure of the N-terminal 388-residue exonuclease fragment of T4 polymerase has been solved as has that of the related RB69 polymerase structure (*9, 10*). The fragment shows very strong structural similarity to that of the 3′−5′ exonuclease domain of the Klenow fragment (KF) of the *Escherichia coli* DNA polymerase (*11*). Given its striking sequence overlap with eukaryotic, human, and other viral DNA polymerases (*12*), the T4 DNA polymerase likely shares a similar structure with all other DNA polymerases (reviewed in ref *13*) folding into two domains, with the C-terminal portion containing the polymerase active site and the N-terminal segment containing the exonuclease active site. Evidence from amber mutants and site-directed mutagenesis (*14*−*17*) and limited proteolysis studies (*18*) also support this bipartite structure for T4 DNA polymerase. Substrate mapping studies showed a separation of two or three nucleotides between the polymerase and exonuclease active sites of T4 DNA polymerase (*19*) with the DNA able to shuttle back and forth between the two sites without re-entering solvent (*20*). However, little is presently known about how DNA is bound and positioned in the two sites or is transferred between them or about what residues are involved in the transfer between the two sites.

Mutant DNA polymerases in which the balance between the polymerase and exonuclease activities is disturbed, leading to an altered mutation frequency, are a preferred system for the examination of such questions. Those polymerases which exhibit a higher ratio of exonuclease to polymerase activity compared with the wild type, and consequently a lower mutation frequency in vivo (*21*), are known as antimutators.

The A737V mutant, previously identified as *ts*CB120 and *ts*L141, was originally discovered as a temperature-sensitive point mutant of bacteriophage T4 (*22*). Bacteriophage T4 carrying this mutated polymerase showed a decreased spontaneous mutation rate (*19*) and an extremely high demand for dNTPs (*23*). If a strong conservation in structure

† Supported by grants from the National Institutes of Health (GM13306).

* To whom correspondence should be addressed. Telephone: (814) 865-2882. Fax: (814) 865-2973. E-mail: sjb1@psu.edu.

‡ The Pennsylvania State University.

§ Current address: Department of Microbiology, Bristol-Myers Squibb Co. Pharmaceutical Research Institute, 5 Research Parkway, Wallingford, CT 06492.

|| National Institute of Diabetes, Digestive & Kidney Diesease.

10.1021/bi980835a CCC: $15.00
Published on Web 10/01/1998

13T/20mer:

```
5'   -TCGCAGCCGTCCAT
3'   -AGCGTCGGCAGGTTCCCAAA
```

13/20-mer:

```
5'   -TCGCAGCCGTCCA
3'   -AGCGTCGGCAGGTTCCCAAA
```

31-mer:

```
5'   -GCCTCGCAGCCGTCCAACCAACTCATTTTTT
```

Trap (13thio/20temp):

```
5'   -AGCGCATTGCTGC[a]
3'   -TCGCGTAACGACGGCAGGAA
```

[a] where ***T, G & C*** are the corresponding thionucleotides.

FIGURE 1: Sequences of DNA substrates and trap used in the kinetic study.

is presumed between T4 and RB69 in the "thumb" region the polymerase, valine 737 would lie close to the DNA found in the exo site. Previous biochemical characterization of the antimutator polymerase A737V suggested that the balance between polymerase and exonuclease activity had been shifted toward increased proofreading in the mutants (*24*−*27*). More recently, Spacciapoli and Nossal (*28*) hypothesized that DNA moves more readily from the polymerase to the exonuclease site in the A737V mutant polymerase. This idea can be directly tested by pre-steady-state kinetics, which is capable of determining the rate constants for the individual steps along the reaction pathway, including the rates of switching between the polymerase and exonuclease sites.

We report pre-steady-state and steady-state kinetic analyses used to investigate the behavior of the antimutator A737V to distinguish between a number of explanations for its antimutator behavior. The determined kinetic sequence was compared to that for the wild-type enzyme and has provided insights into the dynamics of proofreading by this enzyme.

EXPERIMENTAL PROCEDURES

Materials

Radionucleotides, [α-^{32}P]dATP and [γ-^{32}P]ATP, were purchased from New England Nuclear. Ultrapure, unlabeled dNTPs were obtained from Pharmacia. Oligonucleotides (Figure 1) were synthesized using the Expedite Nucleic Acid Synthesis System, and were purified as previously described (*1*) except that the oligonucleotides were resuspended in TE buffer [10 mM Tris·HCl (pH 7.5) and 1 mM EDTA]. Duplexes (13/20-mer and 13T/20-mer) were prepared by annealing equimolar quantities of the single strands in TE buffer and purifying away any residual single-strand material on 3 mm nondenaturing (20% acrylamide/TBE) gels. They were recovered (*1*) and resuspended in TE buffer. Duplex levels were quantitated as indicated by Kuchta et al. (*29*) through a 5′-^{32}P-end label (*30*). The DNA trapping agent (13thio/20temp, see Figure 1) was synthesized using the sulfurizing reagent purchased from Glen Research, employing the same protocol used for normal oligonucleotides. All other chemicals were of the highest purity commercially available. The water used was distilled and deionized.

The wild-type T4 and A737V polymerases were purified as described in ref *28*. *E. coli* DNA polymerase Klenow fragment (KF) was purified as described previously (*31*).

Methods

Kinetic Analysis. All kinetic experiments were carried out in an assay buffer consisting of 67 mM Tris·HCl (pH 8.8), 10 mM 2-mercaptoethanol, and 60 mM NaCl, at 20 °C unless stated otherwise. The sequences of the 13/20-mer, 13thio/20temp, and 13T/20-mer primer−template structures and single-stranded 31-mer are shown in Figure 1. All rapid quench studies were performed with the instrument described by Johnson (*32*). Concentrations are final concentrations unless noted.

Active Site Titration of the Mutant Polymerases. Rapid quench experiments were performed by mixing a solution containing the mutant T4 polymerase (50 nM, as determined with an E_{280} of 130 120 M^{-1} cm^{-1}), 5′-^{32}P end-labeled 13/20-mer (500 nM), and EDTA (0.1 mM) in assay buffer, with an equal volume of a solution containing $MgCl_2$ (10 mM) and dATP (100 μM) in assay buffer. The reaction was terminated at various times (5−1000 ms) by the addition of EDTA (0.25 M). A 10 μL aliquot was removed at each time point and combined with 10 μL of gel loading buffer (90% formamide, 1× TBE, 0.25% bromophenol blue, and 0.25% xylene cyanol). Samples (8 μL) were separated on a denaturing gel (20% acrylamide/8 M urea/TBE). Products were then visualized and quantitated using the Molecular Dynamic Phosphorimager and ImageQuant software version 3.3.

Idling Turnover. Idling turnover was performed at room temperature in the presence of 13/20-mer DNA (1 μM), T4 DNA polymerase (40 nM), $MgCl_2$ (10 mM), and [α-^{32}P]-dATP (300 μM, 250 cpm/pmol) in assay buffer. At reaction times of up to 30 min, samples (5 μL) were withdrawn from the reaction mixture (100 μL total) and the reactions quenched into 10 μL of EDTA (0.1 M). The quenched samples were spotted (1 μL) onto a PEI-cellulose TLC plate, and the plate was developed with potassium phosphate (0.3 M, pH 7.0). The dATP and dAMP bands were visualized and quantitated as described previously (*1*).

Determination of Exonuclease Activity on 31-mer. T4 DNA polymerase (500 nM) was preincubated with 31-mer single-stranded DNA (100 nM) before the initiation of reaction by addition of an equal volume of $MgCl_2$ (7 mM) in assay buffer. The reaction was terminated by quenching into 0.5 M EDTA, and the products were analyzed as described above.

Determination of Exonuclease Activity on 13T/20-mer. For reactions performed with excess DNA over enzyme, a solution of 13T/20-mer (500 nM) and A737V (100 nM) was mixed with $MgCl_2$ (7 mM) in assay buffer. The reactions were quenched with EDTA (0.5 M), and the products were analyzed as described above. For reactions with excess enzyme over DNA, the same procedure was performed except the initial concentrations of 13T/20-mer and A737V mutant polymerase were 100 and 500 nM, respectively. Alternatively, a solution of the A737V mutant polymerase (100 nM) was mixed with a second solution of 13T/20-mer

Scheme 1: Kinetic Scheme for DNA Duplex Crossover between Exonuclease and Polymerase Activities in A737V Mutant Polymerase

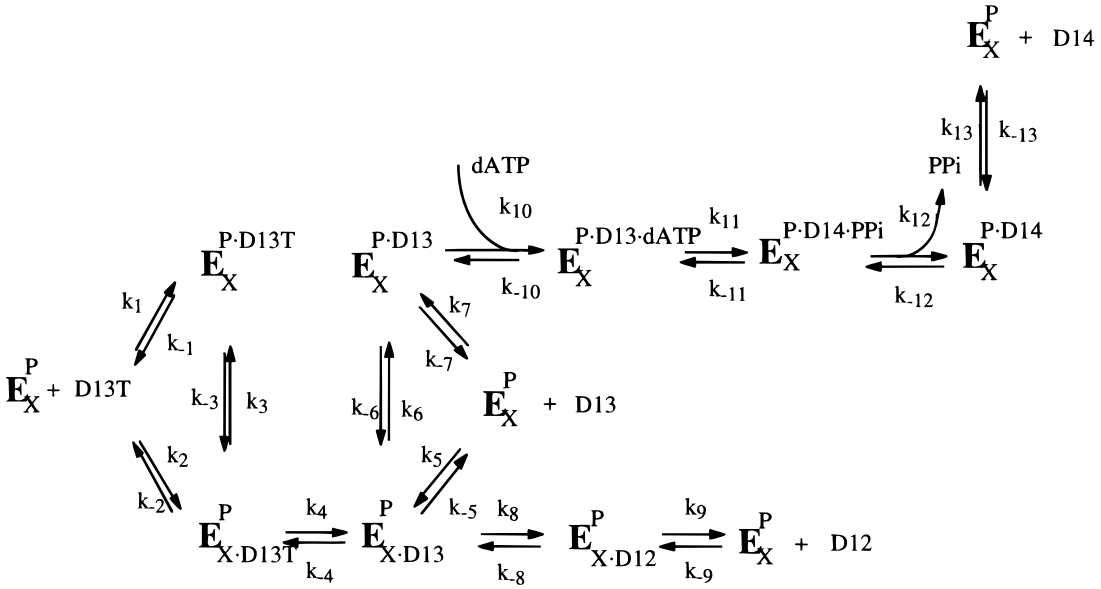

(500 nM) and $MgCl_2$ (7 mM) in assay buffer. The reactions were quenched and analyzed as described above.

Determination of the A737V Polymerase−DNA Dissociation Rate Constant. The 5′-^{32}P end-labeled 13/20-mer (100 nM) was preincubated with an excess of A737V mutant polymerase (500 nM) in one syringe and the solution mixed with an equal volume of unlabeled 13thio/20temp (sequence shown in Figure 1) at three different concentrations (10, 15, and 20 μM). The mixture was incubated for varying amounts of time (5−20000 ms) and chased with $MgCl_2$ (10 mM) and dATP (100 mM), and then the reaction was quenched after 50 ms with EDTA (0.5 M).

Methods for Measuring Duplex Crossover between the Exonuclease and Polymerase Sites. T4 DNA polymerase (500 nM) and 13T/20-mer (100 nM) were preincubated and then mixed with $MgCl_2$ (10 mM) and [α-^{32}P]dATP (50 μM, 2500 cpm/pmol). A second reaction was performed in which 13thio/20temp trap (20 μM) was included in the Mg^{2+}/dATP solution to bind free polymerase. A third reaction, to check the efficiency of trapping of the polymerase, was performed with the 13thio/20temp (20 μM) present in both the enzyme/DNA mixture and the Mg^{2+}/dATP solution (pretrapping). Reactions were terminated at varying times (5−1000 ms) by quenching into EDTA (0.25 M). Aliquots from each time point were spotted in triplicate onto DE-81 paper and washed as described previously (*29*). The efficiency of binding of duplex DNA to DE-81 was determined by spotting known quantities of 5′-^{32}P-labeled 13T/20-mer and washing as indicated above.

Analysis of the Products from the Crossover Experiment. The experiment was performed under the same conditions as the original crossover experiment except that the 13T/20-mer was 5′-^{32}P end-labeled, while the dATP carried no label and dGTP (50 mM) was also included in the assay. The reaction was terminated and analyzed as described previously.

Analysis of the Products of Idling Turnover. An idling turnover experiment was carried out to check the products present in the reaction mixture. The reaction conditions were the same as in original idling turnover experiment except that 13/20-mer was 5′-^{32}P end-labeled while dATP carried no label. The reaction was terminated and analyzed as described above.

Data Analysis. The nonlinear regression analysis of the rate profiles was performed with the program RS1 (BBN Software Products Corp.) run on a mini-VAX machine. The simulations of the kinetic data were done with the program KINSIM (*33*) as modified by Anderson et al. (*34*).

RESULTS

Active Site Titration. In addition to UV measurements of concentration, active site titrations were performed to assess the concentration of active enzyme. The enzyme was provided with only the next correct nucleotide, limiting the reaction to a single base incorporation per substrate molecule. For the 13/20-mer DNA, substrate dATP is the next correct nucleotide to be incorporated, converting the 13/20-mer to a 14/20-mer product. The normal time course of dATP incorporation should be biphasic, consisting of an initial burst phase followed by a second slower phase where the burst amplitude corresponds to the number of enzyme−DNA complexes formed during the preincubation. Under conditions of saturating DNA concentrations, the concentration of enzyme−DNA complexes is equivalent to the concentration of the active enzyme. The two methods gave very similar results with the wild-type and two other T4 mutant polymerases (L771F and A737V/L771F, unpublished results). However, the A737V enzyme has a much slower polymerization rate so there were no distinct fast and slow phases in the active site titration as described later. This behavior reflects a change in the partitioning of the DNA between polymerase and exonuclease sites and could be computer simulated from the rate constants k_5 and k_{-5} through k_{13} and k_{-13} in Scheme 1 and Table 1. In the following kinetic studies, the concentration of A737V was determined solely through the use of A_{280} measurements.

Idling Turnover. Idling turnover features a cycle of nucleotide incorporation followed by excision. In this

Table 1: Kinetic Parameters Used in Simulations of Polymerase and Exonuclease Activity of A737V T4 DNA Polymerase

k_1	2.0×10^8 M^{-1} s^{-1}	k_{-1}	14 s^{-1} [a]	K_d	70 nM[e]
k_2	5.7×10^8 M^{-1} s^{-1}	k_{-2}	20 s^{-1} [b]	K_d	35 nM[e]
k_3	3 s^{-1} [c]	k_{-3}	6 s^{-1} [c]		
k_4	20 ± 10 s^{-1} [d]	k_{-4}	0 s^{-1} [d]		
k_5	4.27×10^7 M^{-1} s^{-1}	k_{-5}	20 s^{-1} [a]	K_d	468 nM[e]
k_6	20 ± 10 s^{-1} [f]	k_{-6}	2.8 ± 1.4 s^{-1} [f]		
k_7	2.0×10^8 M^{-1} s^{-1}	k_{-7}	14 s^{-1} [a]	K_d	70 nM[e]
k_8	20 ± 10 s^{-1} [d]	k_{-8}	0 s^{-1} [d]		
k_9	20 s^{-1}	k_{-9}	4.27×10^7 M^{-1} s^{-1}	K_d	468 nM[e]
k_{10}	1.0×10^8 M^{-1} s^{-1}	k_{-10}	2000 s^{-1}	K_d	20 μM[e]
k_{11}	100 s^{-1} [e]	k_{-11}	0.5 s^{-1} [e]		
k_{12}	2000 s^{-1}	k_{-12}	1×10^5 M^{-1} s^{-1}	K_d	20 mM[e]
k_{13}	14 s^{-1} [a]	k_{-13}	2.0×10^8 M^{-1} s^{-1} [a]	K_d	70 nM[e]
k_{14}	20 s^{-1}	k_{-14}	4.27×10^7 M^{-1} s^{-1}	K_d	468 nM[e]
k_{15}	20 ± 10 s^{-1} [f]	k_{-15}	2.8 ± 1.4 s^{-1} [f]		

[a] In the crossover experiment, the k_{off} s of both mismatched and matched DNA from the exonuclease site were assumed to be the same and the rate was determined to be 20 s^{-1}. Since the combined off rate of 13/20-mer from polymerase and exonuclease site was determined to be 15 s^{-1}, and the distribution of the 13/20-mer at the polymerase and exonuclease site is 87 and 13%, respectively, the off rate from the polymerase site was thus calculated to be 14 s^{-1}. [b] From the crossover experiment, the fit of burst amplitude requires a k_{off} from the exonuclease site of 20 s^{-1}. [c] From the exonuclease activity (enzyme in excess) experiment, the rate of switching from the polymerase site to the exonuclease site was determined to be 6 s^{-1}. Since mismatched DNA was distributed in a 2:1 ratio between the exonuclease and polymerase sites, the rate of switching from the exonuclease to polymerase site was calculated to be 3 s^{-1}. [d] The hydrolytic excision rates of both mismatched and matched DNA were assumed to be the same, and the value of 20 ± 10 s^{-1} was from the three exonuclease activity experiments. The observed differences in exonucleolytic turnover between the mismatched and matched DNA were assumed to be due to their differing affinities for the exonuclease site and different rate of switching from the polymerase site to the exonuclease site, not due to the excision rate itself. [e] The K_d of DNA (both matched and mismatched) to the polymerase site was assumed to be the same as that of the wild type. The measured partitioning of DNA between the polymerase and the exonuclease sites allowed K_ds for DNA binding to the exonuclease site to be determined. The rates of polymerization steps 10−12 are derived from analogous steps in the mechanism of the wild-type enzyme, except that the rate of polymerization step k_{11} was set to 100 s^{-1} due to its observed slower polymerase rate. [f] From computer simulation of data in exonuclease activity, crossover, and idling turnover experiments. The ratios of k_6:k_{-6} were held to 87:13.

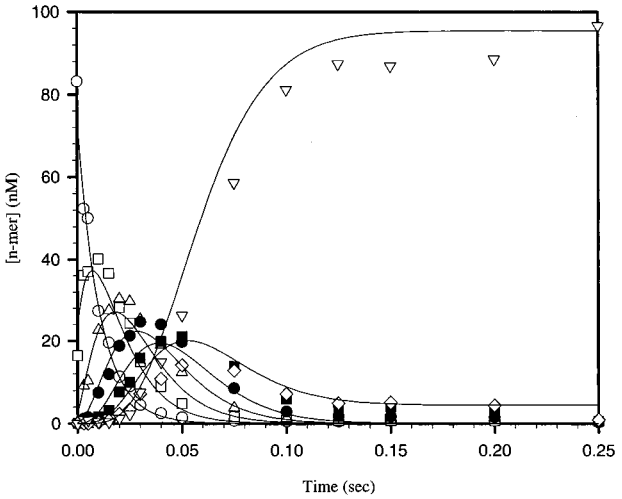

FIGURE 2: Time course of hydrolytic cleavage by the A737V exonuclease of the 31-mer showing the products: 31-mer (○), 30-mer (□), 29-mer (△), 28-mer (●), 27-mer (■), 26-mer (◇), and ≤25-mer (▽). The solid lines were fit to a sequential series of reactions, T4−31-mer → T4−30-mer → ... T4−*N*-mer, with the cleavage rate constant set at 95 s^{-1}.

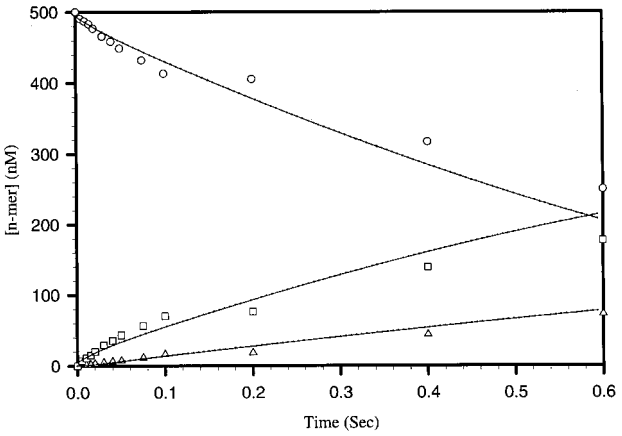

FIGURE 3: Time course of exonucleolytic excision of 13T/20-mer (○) to form 13/20-mer (□) and 12/20-mer (△), with DNA in excess. Excess 13T/20-mer (500 nM) was preincubated with T4 A737V polymerase (100 nM), and the reaction was initiated by addition of $MgCl_2$ (7 mM) and quenched at various times with EDTA (0.5 M). The solid curves were computer simulated from Scheme 1 and rate constants in Table 1.

experiment, dATP was incorporated into 13/20-mer and subsequently dAMP was excised. The rate of dAMP production is a measure of the idling turnover. The nucleotide turnover rate obtained for A737V mutant polymerase was 9-fold higher than that of the wild-type polymerase (data not shown), in agreement with previous reports (*24*, *27*).

Exonuclease Activity on Single-Stranded DNA. Antimutators have a higher exonuclease:polymerase ratio than the wild type (*26*, *27*). To investigate whether this is caused by increased exonuclease activity, single-stranded 31-mer was used as a substrate to avoid the kinetic complexity caused by duplex melting in double-stranded DNA. The rate constant for hydrolytic cleavage (95 s^{-1}) by A737V, as determined by simulation of successive product formation (Figure 2), was almost identical to that of the wild-type enzyme (100 s^{-1}). This result showed that the intrinsic exonuclease activity of the mutant enzyme is unchanged, and the change in the exonuclease:polymerase ratio observed in the idling experiment is likely caused by a change in the rate of switching between the polymerase and exonuclease sites. A similar conclusion was reached with steady-state analysis (*26*, *28*).

Exonuclease Activity on Double-Stranded DNA. One way to examine the partitioning of DNA between the polymerase and exonuclease sites is to monitor exonucleolytic hydrolysis of double-stranded DNA. Incubation of the A737V mutant polymerase with excess 13T/20-mer led to the biphasic formation of 13/20-mer, with a steady-state rate that is faster than that of the wild type. The burst amplitude was ca. 65% (Figure 3), while the burst in the case of the wild type is about 20% (*1*). The burst amplitude should correspond to the amount of DNA initially at the exonuclease site before the remainder switches from a polymerase site to an exonuclease site so the misincorporated nucleotide can be excised. The production of 13/20-mer from the incubation of excess A737V with 13T/20-mer also followed a double-exponential time course. A majority (about 65%) of 13T/20-mer underwent excision at a fast rate (30 s^{-1}) (Figure 4), while 35% of 13T/20-mer was excised at a slower rate of

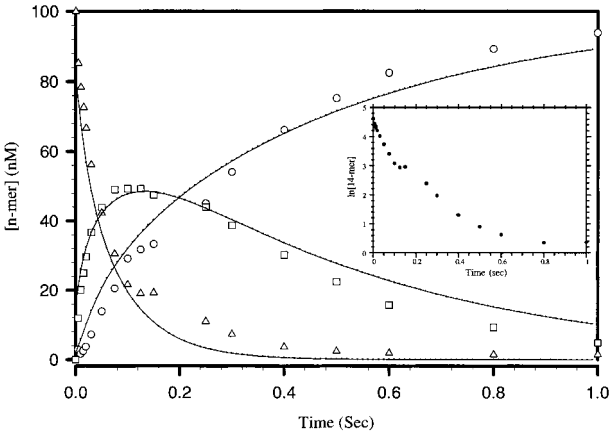

FIGURE 4: Time course of exonucleolytic excision of 13T/20-mer (△) to form 13/20-mer (□) and 12/20-mer (○) with polymerase in excess. Excess A737V polymerase (500 nM) was preincubated with 13T/20-mer (100 nM), and the reaction was initiated by addtion of $MgCl_2$ (7 mM) and quenched at various times with EDTA (0.5 M). The solid curves were computer simulated from Scheme 1 and rate constants in Table 1. The inset more clearly shows the biphasic nature of the time course.

ca. 6 s^{-1}. The logarithimic plot (inset) shows the biphasic nature of the time course more clearly. However, in a similar experiment with wild-type DNA polymerase, significantly more 13T/20-mer was excised at a slower rate than at the faster rate. Both experiments suggested that for A737V, 65% of mismatched DNA binds at the exonuclease site and 35% at the polymerase site. The solid curves were generated by computer simulation of Scheme 1 using the rate constants k_1 and k_{-1} through k_9 and k_{-9} in Table 1.

Examination of Trap Efficiency and Its Effect on Enzyme−DNA Dissociation Rate Constants. Prior to examining the partitioning of DNA between the polymerase and exonuclease sites through a crossover experiment, we conducted experiments to determine the trapping efficiency for enzymes that had dissociated from the DNA substrate. Commonly used trapping reagents include heparin and single-stranded DNAs from salmon sperm and calf thymus. Previous work from this laboratory has shown that heparin affects the k_{off} for the dissociation of the enzyme−DNA complex (*1*). Salmon sperm DNA failed to trap the enzyme efficiently at long times (>200 ms) (data not shown). The double-stranded 13thio/20temp (see Figure 1) successfully functioned as a trap as was confirmed by rapid quench experiments (data not shown) with no leakage of enzyme from the trap duplex for up to 750 ms. Moreover, at three different trap concentrations (10, 15, and 20 mM), the measurement of the rate constant for the dissociation of the enzyme−DNA−13/20-mer complex (15 s^{-1}) showed they were unaffected.

Duplex Crossover between Exonuclease and Polymerase Sites. The crossover experiments were conducted with enzyme bound to 13T/20-mer, and the amount of 13T/20-mer correctly edited and extended to 14/20-mer was measured. The burst amplitude of 14/20-mer in the presence of trap is ca. 12% of the total DNA (data not shown). Since T4 DNA polymerase has a very high replication fidelity, nucleotides are generally not added onto a DNA primer containing a mismatch so that the mismatched dTMP of 13T/20-mer has to be excised at the exonuclease site before dAMP can be incorporated into the primer. The burst amplitude should reflect the percentage of mismatched DNA residing at the exonuclease site that is transferred to the polymerase without dissociation. The burst amplitude of 12% was generated by computer simulation of Scheme 1 from the rate constants in Table 1 (steps k_8 and k_{-8} and k_9 and k_{-9} were omitted) after further kinetic analysis of the fits of the requisite E−DNA complexes.

Analysis of the Products of Crossover. To address the discrepancy between the results from the crossover and the exonucleolytic excision experiments (12% of the mismatched DNA is excised, transferred to the polymerase site, and extended vs 65% of the bound mismatched DNA that is excised), an experiment was performed to check the products from the crossover. In the crossover experiment, it was assumed that once the mismatched dTMP was excised at the exonuclease site, the DNA switched directly to the polymerase site without dissociation from the exonuclease site. Since only the 14-mer, which contained [^{32}P]dAMP, could be traced while the excision products were not, this assumption was not tested. To trace both the excised and extended products, the experiment was repeated under the same conditions except that 13T/20-mer was 5′-labeled with ^{32}P, while dATP and dGTP carried no label. The dGTP was included to distinguish between 13T-mer and 14-mer. Once the 14-mer was formed, it would be further extended to a 17-mer in the presence of dGTP, since the next three nucleotides to be incorporated are dGTP. The results (data not shown) showed that 15% of the duplex was present as the 13/20-mer, consistent with dissociation of 13/20-mer from the exonuclease active site before switching to the polymerase site. In comparison, there is <7% dissociation of 13/20-mer from the wild-type enzyme in an identical experiment. Like 13/20-mer, 13T/20-mer can also dissociate from the exonuclease site so that the direct dissociation of substrate from the exonuclease site in the form of both the 13T/20-mer and the 13/20-mer contributes to the low burst amplitude observed in the crossover experiment with A737V polymerases.

Analysis of the Products of Idling Turnover. The dissociation of DNA from the exonuclease site was also investigated through analysis of the products of idling turnover. The experiment was carried out as described previously except that 13/20-mer was 5′-labeled with ^{32}P while dATP carried no label. We found 87% of DNA was present at the steady state as 14/20-mer and 13% as 13/20-mer (data not shown). The ratio of 14/20-mer to 13/20-mer produced reflects the partitioning of the DNA duplex between the polymerase and exonuclease sites in the steady state. This is confirmed by computer simulation of the data using Scheme 2 and the rate constants in Table 1 which provided a steady-state level of 14/20-mer of ca. 90%.

Accessibility of the Exonuclease Site (E vs D Experiment). Since there is apparent dissociation of DNA directly from the exonuclease site to solution, confirmation for direct access by DNA to the exonuclease site from solution was sought. An experiment was performed under conditions identical to those of the exonuclease activity experiments described above, except that A737V and 13T/20-mer were in separate solutions before mixing to initiate the reaction. Because a burst of 13/20-mer (ca. 65%) was also observed in this experiment, there is direct access to the exonuclease site from

Scheme 2: Kinetic Scheme for the Idling Turnover Process by A737V Mutant Polymerase

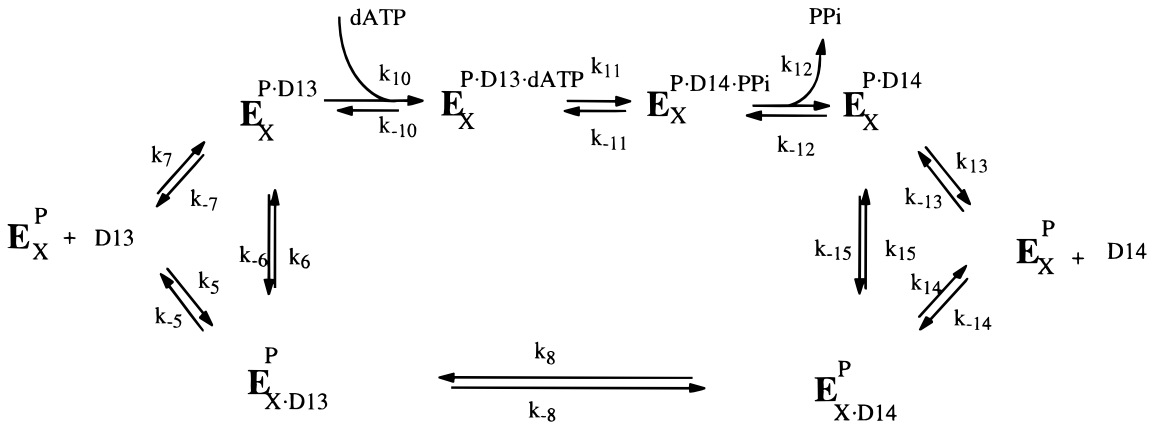

solution. No burst was detected with the wild-type enzyme (*1*).

DISCUSSION

The above results form the basis for a kinetic sequence for the A737V antimutator polymerase that is substantially different in some aspects from that of the wild-type enzyme. The sequence identifies individual steps in DNA replication that are affected by the A737V mutation, which confer antimutator activity. The differences between the two enzymes are most apparent in studies in which the properties of the exonuclease site are examined.

Idling turnover experiments showed that A737V has an 8.7-fold higher nucleotide turnover rate than that of the wild type, which agrees with the observation of Gillin and Nossal (*26*). Examination of the exonuclease activity, however, using single-stranded DNA (31-mer) showed that the exonucleolytic rate is the same as that for the wild type, so a higher intrinsic exonuclease activity is not responsible for increased nucleotide turnover. A similar conclusion was reached by Spacciapoli and Nossal (*28*). The greater activity could be caused by a disturbance in the partitioning of the DNA between the polymerase and exonuclease activities in the antimutator, resulting in a higher proportion of DNA residing at the exonuclease site.

To test this hypothesis, the exonuclease activity on double-stranded DNA (13T/20-mer) was measured with excess DNA over enzyme. The initial burst of the biphasic kinetics corresponds to the proportion of mismatched DNA at the exonuclease site, which for A737V is 65 ± 10%, compared to <20% for the wild type. A converse experiment, using excess enzyme over DNA, showed that excision from 13T/20-mer followed a double-exponential curve. The fast portion of this curve corresponds to 61 ± 7% of total DNA. Both these results are entirely consistent with our hypothesis.

To further examine the fate of 13T/20-mer bound at the exonuclease site, crossover experiments were performed with the A737V mutant enzyme. The burst amplitude here is a measure of the proportion of DNA residing at the exonuclease active site that, after excision, is transferred to and extended at the polymerase site. It was anticipated from the previous results that the amplitude would approximate 65% and not the 12% that was observed. The most reasonable explanation for this anomaly would be dissociation of the substrate DNA from the exonuclease site of the mutant directly into solution.

To demonstrate that DNA dissociates from the exonuclease site in the A737V mutant enzyme, the products of both excision and extension from the crossover reaction were analyzed. We found 14 ± 1% of the 13T/20-mer was extended to 15-, 16-, and 17/20-mers and 15 ± 1% (13/20-mer) dissociated from the exonuclease site before transfer to the polymerase site and subsequent extension. The wild type gave <7% dissociation. The 14% of extended products observed in this experiment correlates very well with the 12% estimated from the burst amplitude. The loss of 13/20-mer, however, only partly accounts for the low burst amplitude relative to that of the wild-type enzyme. Dissociation of the initial 13T/20-mer from the exonuclease site prior to excision also contributes because the rates of dissociation and excision of substrate (k_4 vs k_{-2}) are comparable at the exonuclease site. Consequently, ca. 33% of 13T/20-mer (0.5 × 65%) would dissociate before excision, transfer, and extension took place. Analysis of the products of idling turnover further confirmed the direct dissociation of DNA from the exonuclease site. In the wild-type enzyme, only about 5% of the product is present as 13/20-mer (the product of direct dissociation from the exonuclease site), whereas about 13% is present as 13/20-mer in the mutant, in good agreement with the 15% noted in the crossover experiment. The amount of DNA bound to the enzyme is negligible under steady-state conditions. This shows that dissociation from the exonuclease site is effectively negligible in the wild type, whereas dissociation is significant for the mutant; any kinetic mechanism proposed must take this into account.

Because competing dissociation of the substrate from the exonuclease site had been convincingly demonstrated, we turned our attention to demonstrating direct access from solution to the exonuclease site. Confirmation of direct access to the exonuclease site of A737V was provided by mixing the enzyme and duplex DNA which revealed a burst of 13/20-mer (56 ± 12%). Direct access to the exonuclease site in the wild-type polymerase was not observed, although the outcome of the experiment is compromised by the low occupancy of the exonuclease site. The burst for A737V arises from 13T/20-mer that binds directly to the exonuclease site, and then undergoes excision. This observation has precedent in the studies of Donlin et al. (*35*), on the T7 DNA polymerase, which showed significant accessibility to the exonuclease site.

Previous studies in our laboratory have delineated the kinetic mechanism of wild-type T4 DNA polymerase (*1*). The minimal kinetic scheme for the wild-type enzyme has discrete steps along a pathway for processing mismatched DNA (13T/20-mer). The 13T/20-mer must bind at the polymerase site before it can switch to the exonuclease site, where the misincorporated dTMP is excised. After excision, 13/20-mer switches back to the polymerase site, and nucleotide incorporation resumes. In the wild-type enzyme, mismatched DNA is distributed in a 4:1 ratio between the polymerase and exonuclease sites, with the switching rates in the ratio 20 s^{-1}:5 s^{-1}. Alternatively, this ratio may describe an activation of the duplex for excision by local melting of the duplex followed by rapid excision of the terminal 3′-base. In any case, melting before primer excision is anticipated.

A kinetic scheme (Scheme 1) for the A737V mutant was constructed on the basis of the observations discussed above. Data from Table 1 were used in the computer simulations. These data were determined as follows. The K_ds for steps 1 and 7 for matched and mismatched DNA binding at the polymerase site were set equal to the K_d measured for the wild-type enzyme. This value could not be determined using the usual pre-steady-state active site titration because of the difficulty in assessing the burst amplitude. The K_d value (70 nM) was taken from Capson et al. (*1*). The measured partitioning of mismatched DNA between the polymerase and exonuclease sites (35% vs 65%) allowed calculation of a K_d of 37 nM for step 2. The experimentally determined k_{off} of 15 s^{-1} was a combination of off rates for DNA from polymerase and exonuclease sites. The off rates, k_{-2} and k_{-5}, from the exonuclease site (20 s^{-1}) were determined by fitting data from the crossover experiments and assigned to both matched and mismatched DNA substrates. With the known distribution of 13/20-mer at polymerase and exonuclease sites (87 vs 13%), the off rates from the polymerase site for matched and mismatched DNA substrates (k_{-1} and k_{-7}) were determined to be 14 s^{-1}. The on rates were calculated from K_d and k_{off} values. The switch rates between the polymerase site and exonuclease site in step 6 are also computer simulated on the basis of the distribution of 13/20-mer. The rates of polymerization steps 10−12 are derived from analogous steps in the mechanism of the wild-type enzyme, except that the rate of the polymerization step k_{11} was set to 100 s^{-1}, because Spacciapoli and Nossal (*28*) found the polymerase activity of A737V to be 24% of that of the wild type, which has a polymerization rate of 400 s^{-1}. A substantially lower polymerase rate was also observed in the active site titration experiment and multiple-turnover experiment (data not shown). The excision rate of step 4 was determined from a combination of exonuclease experiments and simulations using Scheme 2.

The completed kinetic scheme was used to examine the proposal of Spacciapoli and Nossal (*28*), based on steady-state data, that the antimutator behavior in A737V is due to more rapid movement of DNA from the polymerase to exonuclease sites. Because of the size of the kinetic scheme and the need to presume that the rate constants for some steps are unchanged from that of the wild-type enzyme, we gauged the sensitivity of the kinetic scheme by arbitrarily changing the partitioning of the DNA between the polymerase and exonuclease sites. The simulations were then compared to the actual collective data. For the key experiments measuring exonuclease activity, idling turnover, or crossover, the data were very sensitive to the distribution of the DNA between the polymerase and exonuclease sites, as imbedded in the rate constant ratios of k_3/k_{-3}, k_6/k_{-6}, and k_{15}/k_{-15}. For example, a 2-fold decrease in k_{-3}/k_3 decreases the amplitude in the crossover experiment by 25%. Similarly, changing the ratio of k_6/k_{-6} (k_{15}/k_{-15}) to 60:40 drops the percentage of 14-mer in the idling experiment by 10% and in the crossover experiment by 25%. We conclude that the reported values reflect the interconversion events between the polymerase and exonuclease sites. For the wild-type enzyme, the rate of passage between pol and exo sites is 1−5 s^{-1} for correct and mismatched DNA and in the reverse direction is 20 s^{-1} for mismatched duplex but minimally >23 s^{-1} for correct DNA. The latter rate has not been determined because there is no evidence for a kinetically significant step for primer repositioning in the polymerase site of the wild-type enzyme after rapid excision. For comparison, the rate of switching for the A737V polymerase between pol and exo sites is 3−6 s^{-1} for correct and mismatched DNA and in the reverse direction is only 3 s^{-1} for mismatched duplex and 20 s^{-1} for correct DNA. Consequently, there is a markedly diminished shuttle rate from exo to pol, and an increased shuttle from pol to exo for the A737V versus wild-type polymerase, so in the case of a 3′-primer terminus mismatch, the DNA is partitioned between the polymerase and exonuclease sites in a 1:2 ratio for A737V and 4:1 ratio for the wild-type enzyme. The result is an enhanced exonuclease activity for the antimutator enzyme. It is noteworthy, however, that although the intrinsic exonuclease activity (100 s^{-1}) toward a single strand of DNA is unchanged for the antimutator, the exonuclease activity toward matched and mismatched duplex is only 20−30 s^{-1}. Whether this lower value reflects an actual effect of the mutation on the processing ability of the exonuclease site, melting of duplex, or results from imprecision in the data is not clear.

From the RB69 polymerase structure, residue A737 in T4 would be located in the thumb region near the N-terminal end of helix T. Four residues of oligo(dT) bound in the exonuclease site were visualized in the crystal structure with the fourth nucleotide from the 3′-end close to S735. It is plausible that by substitution of a larger valine residue in place of A737, the channel crossed by the primer terminus as it switches between the exonuclease and polymerase sites would be affected. It is also possible, in addition, that the substitution of alanine by valine may cause a conformational change which extends into the exonuclease site. Both of these effects would increase the extent of occupation of the exonuclease site by DNA, leading to the observed increase in the exonuclease to polymerase activity ratio, giving rise to higher DNA replication fidelity. The A737V mutations should not influence the rate of exonuclease catalysis, consistent with the finding of comparable rates of hydrolysis of single-stranded DNA of the A737V and wild-type enzyme. These experiments were carried out with the core polymerase and not with the highly processive holoenzyme that results from the association of the polymerase with the gp45, clamp protein (*36*). Increased residence time would alter the outcome of the crossover experiments, but would not change the exonuclease and polymerase site occupancy found for either the wild type or mutant enzymes.

CONCLUSION

It has been conclusively shown by pre-steady-state and steady-state kinetics that the cause of antimutator activity in the A737V T4 DNA polymerase mutant is not increased exonuclease activity. Rather, the effect of the A737V mutation on enzyme activity is primarily to decrease the rate at which DNA is transferred from the exonuclease to the polymerase site. The result is to increase the proportion of DNA residing at the exonuclease site, compared to that of the wild type, leading to the increased proofreading activity observed.

REFERENCES

1. Capson, L. T., Peliska, J. A., Kaboord, B. F., Frey, M. W., Lively, C., Dahlberg, M., and Benkovic, S. J. (1992) *Biochemistry 31*, 10984−10994.
2. Goulian, M., Lucas, Z. T., and Kornberg, A. (1968) *J. Biol. Chem. 243*, 627−638.
3. Huang, W. M., and Lehman, I. R. (1972) *J. Biol. Chem. 247*, 3139−3146.
4. Drake, J. W., Allen, E. F., Forsberg, S. A., Preparata, R.-M., and Greening, E. O. (1969) *Nature 221*, 1128−1132.
5. Loeb, L. A. (1991) *Cancer Res. 51*, 1−5.
6. Kunkel, T. A. (1988) *Cell 53*, 837−840.
7. Goodman, M. F., Creighton, S., Bloom, L. B., and Petruska, J. (1993) *Crit. Rev. Biochem. Mol. Biol. 28*, 83−126.
8. Schaaper, R. M. (1993) *J. Biol. Chem. 268*, 23762−23765.
9. Wang, J., Yu, P., Lin, T. C., Konigsberg, W. H., and Steitz, T. A. (1996) *Biochemistry 35*, 8110−8119.
10. Wang, J., Sattar, A. K. M. A., Wang, C. C., Karam, J. D., Konigsberg, W. H., and Steitz, T. A. (1997) *Cell 89*, 1087−1099.
11. Ollis, D. L., Brick, P., Hamlin, R., Xuong, N. G., and Steitz, T. A. (1985) *Nature 313*, 762−766.
12. Braithwaite, D. K., and Ito, J. (1993) *Nucleic Acids Res. 21*, 787−802.
13. Joyce, C. M., and Steitz, T. A. (1994) *Annu. Rev. Biochem. 63*, 777−822.
14. Nossal, N. G., and Hershfield, M. S. (1971) *J. Biol. Chem. 246*, 5414−5426.
15. Reha-Krantz, L. J. (1988) *J. Mol. Biol. 202*, 711−724.
16. Reha-Krantz, L. (1994) in *Molecular Biology of Bacteriophage T4* (Karam, J. D., Ed.) pp 307−312, American Society for Microbiology, Washington, DC.
17. Frey, M. W., Nossal, N. G., Capson, T. L., and Benkovic, S. J. (1993) *Proc. Natl. Acad. Sci. U.S.A. 90*, 2579−2583.
18. Lin, T. C., Karam, G., and Konigsberg, W. H. (1994) *J. Biol. Chem. 269*, 19286−19294.
19. Gopalakrishnan, V., and Benkovic, S. J. (1994) *J. Biol. Chem. 269*, 21123−21126.
20. Reddy, M. K., Weitzel, S. E., and von Hippel, P. H. (1992) *J. Biol. Chem. 267*, 14157−14166.
21. Drake, J. W. (1991) *Proc. Natl. Acad. Sci. U.S.A. 88*, 7160−7164.
22. Epstein, R. H., Bolle, A., Steinberg, C. M., Kellenberger, E., Boy de la Tour, E., Chevalley, R., Edger, R. S., Susman, M., Denhardt, G. H., and Lielausis, A. (1963) *Cold Spring Harbor Symp. Quant. Biol. 28*, 375−392.
23. Stocki, S. A., Nonay, R. L., and reha-Krantz, L. J. (1995) *J. Mol. Biol. 254*, 15−28.
24. Muzyczka, N., Poland, R. L., and Bessman, M. J. (1972) *J. Biol. Chem. 247*, 7116−7122.
25. Lo, K.-Y., and Bessman, M. J. (1976) *J. Biol. Chem. 251*, 2475−2479.
26. Gillin, F. D., and Nossal, N. G. (1976) *J. Biol. Chem. 251*, 5219−5224.
27. Gillin, F. D., and Nossal, N. G. (1976) *J. Biol. Chem. 251*, 5225−5232.
28. Spacciapoli, P., and Nossal N. G. (1994) *J. Biol. Chem. 269*, 438−446.
29. Kuchta, R. D., Mizrahi, V., Benkovic, P. A., Johnson, K. A., and Benkovic, S. J. (1987) *Biochemistry 26*, 8410−8427.
30. Mizrahi, V., Benkovic, P. A., and Benkovic, S. J. (1986) *Proc. Natl. Acad. Sci. U.S.A. 83*, 5767−5772.
31. Frey, M. W., Sowers, L. C., Millar, D. P., and Benkovic S. J. (1995) *Biochemistry 34*, 9185−9192.
32. Johnson, K. A. (1986) *Methods Enzymol. 134*, 667−705.
33. Barshop, B. A., Wrenn, R. F., and Freiden, C. (1983) *Anal. Biochem. 130*, 134−145.
34. Anderson, K., Sikorski, J. A., and Johnson, K. A (1988) *Biochemistry 27*, 7395−7406.
35. Donlin, M. J., Patel, S. S., and Johnson, K. A. (1991) *Biochemistry 30*, 538−546.
36. Sexton, A. J., Berdis, A. J., and Benkovic, S. J. (1997) *Opin. Chem. Biol. 1*, 316−322.

BI980835A